Available online at www.sciencedirect.com

ScienceDirect

Ceramics International 39 (2013) 9201–9206

CERAMICS INTERNATIONAL

www.elsevier.com/locate/ceramint

Dielectric properties of giant permittivity $NaCu_3Ti_3NbO_{12}$ ceramics

Yang Liu[a,b], Wenchao Wang[c], Jiquan Huang[a], Fei Tang[a,b], Chen Zhu[c], Yongge Cao[a,c,*]

[a]*Key Laboratory of Optoelectronic Materials Chemistry and Physics, Fujian Institute of Research on the Structure of Matter, Chinese Academy of Sciences, Fuzhou 350002, PR China*

[b]*University of the Chinese Academy of Sciences, Beijing 100039, China*

[c]*Department of Physics, Renmin University of China, Beijing 100872, China*

Received 30 March 2013; received in revised form 8 April 2013; accepted 6 May 2013
Available online 14 May 2013

Abstract

A series of $NaCu_3Ti_3NbO_{12}$ ceramics was fabricated by the conventional solid-state reaction method, and their microstructures, phase structures, electric and dielectric properties were systematically investigated. Single phase of $NaCu_3Ti_3NbO_{12}$ with body-centered cubic perovskite-related structure was confirmed by X-ray diffraction. Normal grain growth was observed, and the average size of grains was limited to less than 6 μm. Impedance spectroscopy analysis reveals that $NaCu_3Ti_3NbO_{12}$ ceramics are electrically heterogeneous, consisting of semiconducting grains and insulating grain boundaries. The activation energy for the dc conduction process is comparable to that for conduction at the grain boundaries, indicating that the dc conduction process is associated with the electric response of grain boundaries in $NaCu_3Ti_3NbO_{12}$ ceramics. The dielectric properties can be well described by the internal barrier layer capacitor effect based on Maxwell–Wagner polarization at grain boundaries.

Keywords: C. Dielectric properties; D. Perovskite; IBLC effect

1. Introduction

Dielectric materials with high dielectric constant (ε') and low dielectric loss ($\tan\delta$) are considerably favored and welcomed, because they may have potential to enhance electric performance and shrink reasonable sizes for use in many electronic applications such as capacitors, memories, and filters [1–3]. The cubic perovskite-related oxide $CaCu_3Ti_4O_{12}$ (CCTO) has attracted considerable attention in the past decade, due to its high and nearly temperature independent ε' over a wide temperature range (100–600 K) [4,5]. Many mechanisms have been proposed to explain the origin of dielectric response in CCTO, such as the Cu deficiency model, the internal domains model, the nanoscale disorder model, and the internal barrier layer capacitor (IBLC) model [6–9]. Among them, the most widely accepted mechanism is the IBLC model, which states that the giant dielectric response in CCTO ceramics is attributed to a special electrically heterogeneous microstructure, i.e., thin insulating grain boundaries (GBs) and large semiconducting grains. However, the comprehensive and accurate explanation is still controversial.

In order to further clarify the origin of dielectric response in CCTO and obtain more kinds of CCTO-like materials with outstanding dielectric properties, many oxides which have both compositional and structural similarities with CCTO, such as $SrCu_3Ti_4O_{12}$, $Bi_{2/3}Cu_3Ti_4O_{12}$, $Ca_{1-x}La_{2x/3}Cu_3Ti_4O_{12}$, $Ca_{1-3x/2}Gd_xCu_3Ti_4O_{12}$ and $Na_{1/2}Y_{1/2}Cu_3Ti_4O_{12}$, have been extensively developed [5,10–13]. Recently, several $NaCu_3Ti_3BO_{12}$ (B=Sb, Ta, and Nb) materials with perovskite-related structure have also been reported. It is found that both $NaCu_3Ti_3SbO_{12}$ and $NaCu_3Ti_3TaO_{12}$ possess giant ε' values [14,15]. However, up to date, the dielectric properties of $NaCu_3Ti_3NbO_{12}$ (NCTNO) ceramics have not been reported. In this paper, based on the successful fabrication of NCTNO ceramics via

*Corresponding author at: Chinese Academy of Sciences, Fujian Institute of Research on the Structure of Matter, Key Laboratory of Optoelectronic Materials Chemistry and Physics, 155 Yangqiao Road West, Fuzhou 350002, China. Tel.: +86 591 83721039; fax: +86 591 83713291.
E-mail address: caoyongge@fjirsm.ac.cn (Y. Cao).

0272-8842/$ - see front matter © 2013 Elsevier Ltd and Techna Group S.r.l. All rights reserved.
http://dx.doi.org/10.1016/j.ceramint.2013.05.023

the conventional solid-state reaction method, their dielectric and electric properties in wide ranges of frequency and temperature were investigated, and the possible origin of giant dielectric response was discussed.

2. Experiment details

NCTNO ceramics were fabricated by the conventional solid-state reaction method. Na_2CO_3 (99.99% purity), CuO (99% purity), TiO_2 (99.99% purity), and Nb_2O_5 (99.99% purity) were employed as starting raw materials. Each stoichiometric mixture of the starting materials was ball-milled in ethanol for 24 h. The mixed slurries were dried and then calcined at 950 °C for 10 h. The resulting powders were ground and pressed into pellet disks of 10 mm in diameter and 1 mm in thickness by uniaxial compression at 30 MPa and subsequently cold isostatic pressing (CIP) at 200 MPa. The green bodies were sintered at 1060–1080 °C for 10 h respectively, and then cooled to room temperature naturally.

The phase structure was confirmed by X-ray diffraction (XRD) (MiniFlex-II, Rigaku), the microstructure and composition were characterized by scanning electron microscopy (SEM) with energy dispersive spectroscopy (EDS) (JSM-6700F, JEOL), the electric and dielectric properties were measured using an Agilent 4284 A LCR Meter in the frequency range of 10^2–10^6 Hz and an oscillation voltage of 1.0 V. The measurements were performed at temperatures ranging from 30 °C to 200 °C. Prior to measurements, the ceramic samples were polished. Silver paint was coated onto both faces of the pellets, and fired at 500 °C for 1 h.

3. Results and discussion

Fig. 1 shows the XRD patterns of NCTNO ceramics sintered at different temperatures. The same crystal structure, i.e., a body-centered cubic perovskite-related structure of space group $Im\bar{3}$, was observed in all ceramics. The values of lattice parameter were calculated to be 7.423 Å, 7.425 Å and 7.425 Å for the samples sintered at 1060, 1070 and 1080 °C respectively, which are very close to a value of 7.426 Å reported in the literature [16]. It is also found that the lattice parameter of NCTNO is larger than that of $NaCu_3Ti_3SbO_{12}$ (7.406 Å), which can be ascribed to the larger ionic radius of Nb^{5+} than Sb^{5+} [14]. No impurity phase was observed in all ceramic samples, indicating a successful preparation of single phase NCTNO ceramics.

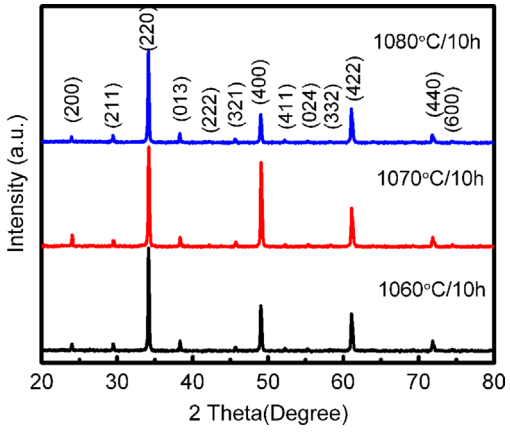

Fig. 1. XRD patterns of NCTNO ceramics prepared under different sintering temperature conditions.

Surface morphology of the NCTNO ceramic sintered at 1070 °C for 10 h is demonstrated in Fig. 2a. Generally, for CCTO and other compositionally/structurally CCTO-like oxide ceramics, abnormal grain growth is very common [12,13,17,18]. However, for NCTNO, as shown in Fig. 2a, dense microstructure was obtained, and the average size of grains was limited to less than 6 μm. Moreover, it is found that the sintering temperatures have little effect on the microstructure when NCTNO ceramics were sintered at 1060–1080 °C

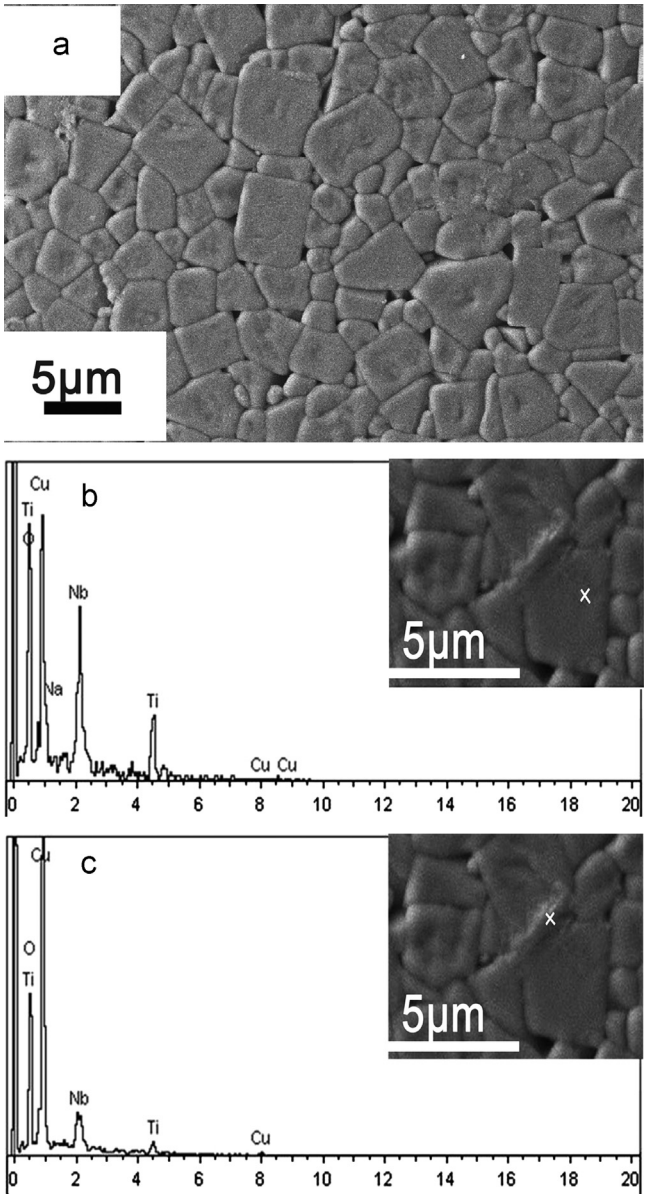

Fig. 2. (a) Surface morphology of the NCTNO ceramic sintered at 1070 °C and EDS spectrum of the NCTNO ceramic detected at (b) grain and (c) GB regions.

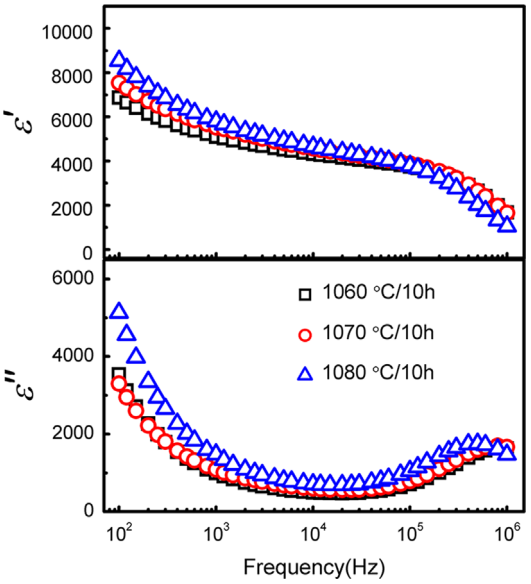

Fig. 3. Dielectric dispersion spectra of NCTNO ceramics measured at room temperature.

for 10 h (results are not shown here). Fig. 2b and c shows EDS spectra detected at grain (b) and grain boundary (GB) (c) regions, respectively. Obviously, the GB region is Cu-rich. Generally, the inhomogeneity of chemical composition, e.g., CuO segregation at GBs, is suggested to be responsible for the high permittivity of CCTO and CCTO-like materials [19].

Fig. 3 shows the frequency dependence of dielectric properties measured at room temperature. The ε' of NCTNO ceramics increases slightly and becomes more frequency dependent with increasing sintering temperature. The values of ε' at 10 kHz for the samples sintered at 1060, 1070 and 1080 °C were found to be 4332, 4566 and 4655, respectively. In the frequency range of 10^5–10^6 Hz, a drastic decrease in ε' can be seen. Correspondingly, a relaxation peak (ε'' peak) is observed, and the peak positions of all samples are almost the same. Generally, the dielectric behavior (especially the ε' value) of CCTO ceramics depends greatly on the sintering temperature as their microstructures are very sensitive to sintering conditions, e.g., higher sintering temperature results in larger grain size and consequently higher ε' [20,21]. Herein, it is found that the dielectric behavior of NCTNO ceramics depends weakly on the sintering temperature (as shown in Fig. 3), which can be attributed to their similar microstructures (similar density and mean particle size). Due to their similar dielectric behavior, the ceramic sintered at 1070 °C for 10 h was chosen as the representative to make the further detailed investigation.

Fig. 4 shows the frequency dependence of ε' and tan δ at different temperatures for the NCTNO ceramic sintered at 1070 °C. At low temperature (e.g., < 60 °C), ε' depends slightly on frequency over the range from 10^2 to 10^5 Hz. However, when the temperature is higher than 70 °C, ε' increases with increasing temperature, and strongly depends on frequency, especially in low-frequency range. Similar trend is observed in tan δ, as shown in Fig. 4b. The dielectric

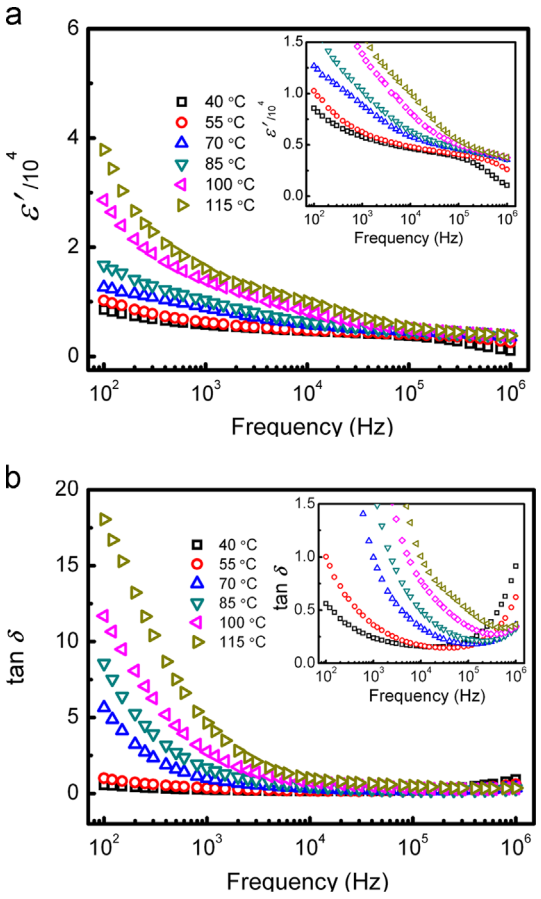

Fig. 4. Frequency dependence of (a) ε' and (b) tan δ at different temperatures for the NCTNO ceramic sintered at 1070 °C.

behavior of NCTNO ceramics (especially at high measured temperature) can be explained by Maxwell–Wagner effect (or interfacial polarization model), which is widely adopted to explain the dielectric relaxation behavior of ceramics with heterogeneous microstructures (e.g., insulating grain with semiconducting GB, semiconducting grain with insulating GB, or insulating matrix with dispersed semiconducting/conducting secondary phase) [22–24]. As mentioned above, the GB region is Cu-rich. Therefore, the dielectric behavior of NCTNO ceramics coincides with this special heterogeneous microstructure. At about 10^5–10^6 Hz, ε' decreases (and tan δ increases) sharply, and the position where this decrease in ε' (and an increase in tan δ) occurs shifts to higher frequency with increasing temperature, indicating a thermal activated high-frequency dielectric relaxation mechanism.

It is widely accepted that the ultra-high permittivity of CCTO and perovskite-related materials originates from the IBLC effect based on Maxwell–Wagner polarization [9,25,26]. Generally, the related electrical properties of grain and GB in such materials can be estimated by an impedance spectroscopy, e.g., the grain resistance (R_g) and GB resistance (R_{gb}) at particular temperatures can be determined by the diameter of two semicircular arcs at high and low frequency ranges, respectively [9,25]. To obtain more information about dielectric properties and clarify the origin of giant ε' response in

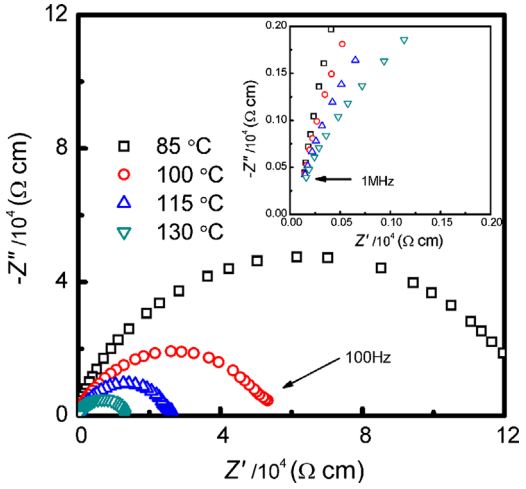

Fig. 5. Impedance complex plane plots for the NCTNO ceramic sintered at 1070 °C; inset shows an expanded view of the high frequency data close to the origin.

NCTNO, its related electrical properties were further studied by an impedance spectroscopy.

Impedance complex plane plots for the NCTNO ceramic at various temperatures are illustrated in Fig. 5. Obviously, only a semicircular arc is observed in the measured frequency range (10^2–10^6 Hz), and the value of a nonzero intercept at high frequencies is very small, indicating the total resistance of NCTNO ceramics is governed by R_{gb}. In other words, $R_{gb} \gg R_g$ (R_{gb} and R_g are the resistances of GB and grain, respectively), and $C_{gb} \gg C_g$ (C_{gb} and C_g are the capacitors of GB and grain, respectively). Therefore, the dielectric properties are mainly determined by the physical characteristics of GB, such as the ε', the resistivity, and the thickness (exactly, the ratio of the average grain size and the GB depletion layer width). Furthermore, it is concluded from the expected diameter of a semicircular arc that the value of R_{gb} decreases with increasing temperature, and presents 3–4 orders of magnitude larger than that of R_g. Therefore, the IBLC effect, as described earlier for CCTO ceramics, can be introduced to describe the dielectric response in NCTNO ceramics, and giant ε' value of NCTNO may be attributed to the effect of special heterogeneous microstructure.

According to the IBLC model based on Maxwell–Wagner polarization, an equivalent circuit model has been considered to analyze the electric properties. The model contains two parallel RC elements (R_gC_g and $R_{gb}C_{gb}$). The element R_gC_g describes the effect of grains, while the element $R_{gb}C_{gb}$ delineates the effect caused by GBs [27]. The complex impedance (Z^*) can be expressed as [9,13]

$$Z^* = \frac{R_g}{1 + i\omega R_g C_g} + \frac{R_{gb}}{1 + i\omega R_{gb} C_{gb}} \tag{1a}$$

Accordingly,

$$Z' = \frac{R_g}{1 + (\omega R_g C_g)^2} + \frac{R_{gb}}{1 + (\omega R_{gb} C_{gb})^2} \tag{1b}$$

and

$$Z'' = R_g \left[\frac{\omega R_g C_g}{1 + (\omega R_g C_g)^2}\right] + R_{gb} \left[\frac{\omega R_{gb} C_{gb}}{1 + (\omega R_{gb} C_{gb})^2}\right] \tag{1c}$$

where ω is the angular frequency.

Fig. 6 reveals the frequency dependence of the imaginary part (Z'') of Z^* at different temperatures for the NCTNO ceramic. With increasing temperature, the peak position of Z'' shifts to higher frequency and the peak intensity decreases, implying a thermally activated electric response, as well as a decrease in the value of R_{gb} with increasing temperature. It is known that $R = 2Z''_{max}$, where Z''_{max} is the maximum value of Z''. Therefore, the values of R_{gb} at different temperatures can be calculated from Fig. 6. As shown in Fig. 7, it is found that the GB conductivity, $\sigma_{gb} = 1/R_{gb}$, follows the Arrhenius law [13,15],

$$\sigma_{gb} = \sigma_0 \exp\left(\frac{-E_{gb}}{k_B T}\right) \tag{2}$$

where σ_0 is the pre-exponential factor, E_{gb} is the activation energy for conduction at the GBs, k_B is the Boltzmann constant and T is the absolute temperature. The value of E_{gb} was calculated to be 0.583 eV, which is comparable to the reported

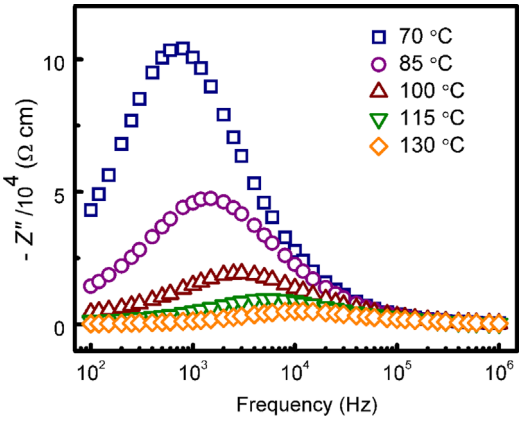

Fig. 6. Frequency dependence of Z'' at different temperatures for the NCTNO ceramic.

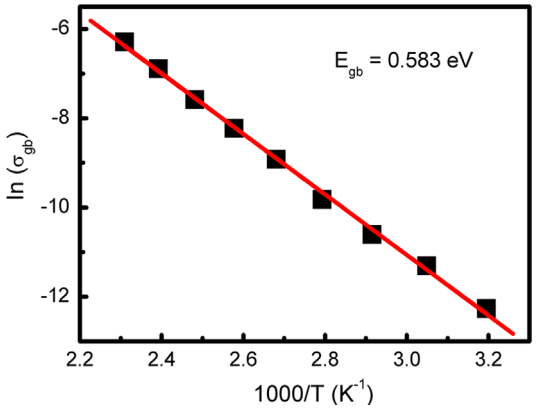

Fig. 7. Arrhenius plot of σ_{gb} for the NCTNO ceramic.

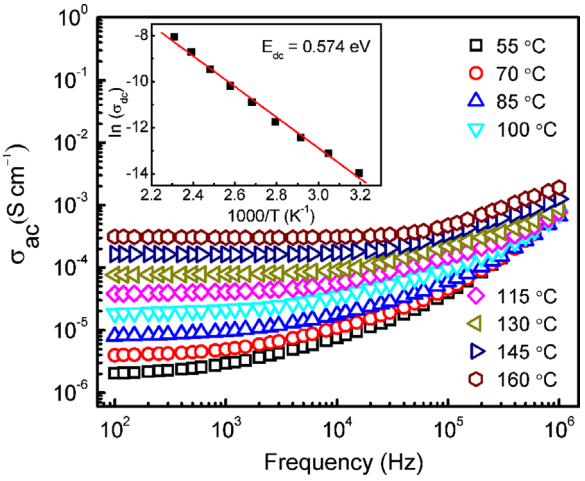

Fig. 8. Frequency dependence of σ_{ac} at different temperatures for the NCTNO ceramic; inset shows Arrhenius plot of σ_{dc}.

values of 0.600, 0.590 and 0.639 eV for CCTO, $La_{2/3}Cu_3Ti_4O_{12}$, and $Na_{1/2}Y_{1/2}Cu_3Ti_4O_{12}$ ceramics, respectively [9,11,14].

To better understand the electric properties of the NCTNO ceramic, the temperature dependence of AC conductivity (σ_{ac}) in the frequency range from 10^2 to 10^6 Hz was also studied, as shown in Fig. 8. Obviously, σ_{ac} exhibits nearly a constant value at low frequencies, and then begins to increase moderately with increasing frequency. This is because electric field does not influence the hopping conduction mechanism when frequency is low. As frequency further increases, electron hopping starts to be active, and no long range motion occurs. Therefore, increase in frequency will lead to increasing electron hopping frequency, and consequently, σ_{ac} increases [12]. It is also found from Fig. 8 that σ_{ac} increases with increasing temperature, which can be attributed to an increase in charge carriers' drift mobility with increasing temperature. Generally, in most solid materials, the total conductivity (σ) is expressed as [12]

$$\sigma = \sigma_{ac} + \sigma_{dc} \tag{3}$$

where σ_{ac} originates from the hopping conduction process, and DC conductivity (σ_{dc}) results from the band conduction process. σ_{ac} is an increasing function of frequency, while σ_{dc} is temperature dependent and frequency independent. AC power law shows the frequency dependence of σ_{ac} [28],

$$\sigma_{ac} = Af^n \tag{4}$$

where A is a constant, f is the frequency, and the exponent n is smaller than 1. As aforementioned, with increasing temperature, σ_{ac} increases and becomes more frequency independent in the low frequency range. This indicates that the low-frequency σ_{ac} can be approximately equal to σ_{dc}, especially at high temperature.

As shown in Fig. 8, the value of σ_{ac} at 100 Hz was used to estimate the value of σ_{dc}. Inset of Fig. 8 presents a plot of ln (σ_{dc}) as a function of reciprocal temperature ($1/T$). It is found that σ_{dc} at different temperatures follows the Arrhenius law [13,29],

$$\sigma_{dc} = \sigma_0 \exp\left(\frac{-E_{dc}}{k_B T}\right) \tag{5}$$

where E_{dc} is the activation energy for the dc conduction process. The calculated E_{dc} was 0.574 eV, which is comparable to E_{gb} (0.583 eV), indicating the dc conduction process is closely associated with the electric response of GBs for the NCTNO ceramic.

4. Conclusion

In conclusion, NCTNO ceramics were fabricated by the conventional solid-state reaction method, and their dielectric and electric properties were studied as functions of frequency and temperature. Microstructure with normal grain growth was observed in NCTNO ceramics. Giant ε' of about 10^4 at room temperature was obtained, which can be attributed to a special heterogeneous microstructure of semiconducting grains and insulating GBs. With increasing temperature, ε' and $\tan\delta$ increased, and became increasingly frequency dependent. The conductivity (σ_{gb}, σ_{ac} and σ_{dc},) increased and the peak position of Z'' shifted to higher frequency, indicating a thermally activated electric response and the IBLC effect based on Maxwell–Wagner polarization at grain boundaries.

Acknowledgments

This work was supported by the National Natural Science Foundation of China (91022035) and the National Natural Science Foundation of China (20901079).

References

[1] C.C. Homes, T. Vogt, S.M. Shapiro, S. Wakimoto, A.P. Ramirez, Optical response of high dielectric constant perovskite-related oxide science, Science 293 (2001) 673–676.
[2] J. Wu, C.W. Nan, Y.H. Lin, Y. Deng, Giant dielectric permittivity observed in Li and Ti doped NiO, Physical Review Letters 89 (2002) 217601-1–217601-4.
[3] J.Q. Huang, H. Zheng, Z.H. Chen, Q. Gao, N. Ma, P.Y. Du, Percolative ceramic composites with giant dielectric constant and low dielectric loss, Journal of Materials Chemistry 19 (2009) 3909–3913.
[4] M.A. Subramanian, D. Li, N. Duan, B.A. Reisner, A.W. Sleight, High dielectric constant in $ACu_3Ti_4O_{12}$ and $ACu_3Ti_3FeO_{12}$ phases, Journal of Solid State Chemistry 151 (2000) 323–325.
[5] M.A. Subramanian, A.W. Sleight, $ACu_3Ti_4O_{12}$ and $ACu_3Ru_4O_{12}$ perovskites: high dielectric constants and valence degeneracy, Solid State Sciences 4 (2002) 347–351.
[6] T.T. Fang, L.T. Mei, Evidence of Cu deficiency: a key point for the understanding of the mystery of the giant dielectric constant in $CaCu_3Ti_4O_{12}$, Journal of the American Ceramic Society 90 (2007) 638–640.
[7] T.T. Fang, C.P. Liu, Evidence of the Internal domains for inducing the anomalously high dielectric constant of $CaCu_3Ti_4O_{12}$, Chemistry of Materials 17 (2005) 5167–5171.
[8] J.C. Zheng, A.I. Frenkel, L. Wu, J. Hanson, W. Ku, E.S. Bozin, S.J. L. Billinge, Y. Zhu, Nanoscale disorder and local electronic properties of $CaCu_3Ti_4O_{12}$: an integrated study of electron, neutron, and X-ray diffraction, X-ray absorption fine structure, and first-principles calculations, Physical Review B 81 (2010) 144203-1–144203-19.

[9] D.C. Sinclair, T.B. Adams, F.D. Morrison, A.R. West, $CaCu_3Ti_4O_{12}$: one-step internal barrier layer capacitor, Applied Physics Letters 80 (2002) 2153–2155.
[10] W.T. Hao, J.L. Zhang, Y.Q. Tan, W.B. Su, Giant dielectric-permittivity phenomena of compositionally and structurally $CaCu_3Ti_4O_{12}$-like oxide ceramics, Journal of the American Ceramic Society 92 (2009) 2937–2943.
[11] S.H. Jin, H.P. Xia, Y.P. Zhang, Effect of La-doping on the properties of $CaCu_3Ti_4O_{12}$ dielectric ceramics, Ceramics International 35 (2009) 309–313.
[12] O.P. Raman Kashyap, R.P. Thakur, Tandon, study of structural, dielectric and electrical conduction behaviour of Gd substituted $CaCu_3Ti_4O_{12}$ ceramics, Ceramics International 38 (2012) 3029–3037.
[13] W. Somphan, N. Sangwong, T. Yamwong, P. Thongbai, Giant dielectric and electrical properties of sodium yttrium copper titanate: $Na_{1/2}Y_{1/2}Cu_3Ti_4O_{12}$, Journal of Materials Science: Materials in Electronics 23 (2012) 1229–1234.
[14] W.T. Hao, J.L. Zhang, Y.Q. Tan, M.L. Zhao, C.L. Wang, Giant dielectric permittivity properties and relevant mechanism of $NaCu_3Ti_3SbO_{12}$ ceramics, Journal of the American Ceramic Society 94 (2011) 1067–1072.
[15] N. Sangwong, W. Somphan, P. Thongbai, T. Yamwong, S. Meansiri, Electrical responses and dielectric relaxations in giant permittivity $NaCu_3Ti_3TaO_{12}$ ceramics, Applied Physics A 108 (2012) 385–392.
[16] B. Rivas-Murias, M. Sánchez-Andújar, J. Rivas, M.A. Senarís-Rodríguez, Influence of high levels of Nb and Ti doping on the dielectric properties of $CaCu_3Ti_4O_{12}$ type of compounds, Materials Chemistry and Physics 120 (2010) 576–581.
[17] S.K. Jo, Y.H. Han, Sintering behavior and dielectric properties of polycrystalline $CaCu_3Ti_4O_{12}$, Journal of Materials Science: Materials in Electronics 20 (2009) 680–684.
[18] P. Thongbai, B. Putasaeng, T. Yamwong, S. Maensiri, Current–voltage nonlinear and dielectric properties of $CaCu_3Ti_4O_{12}$ ceramics prepared by a simple thermal decomposition method, Journal of Materials Science: Materials in Electronics 23 (2012) 795–801.
[19] D. Capsoni, M. Bini, V. Massarotti, G. Chiodelli, M.C. Mozzati, C. B. Azzoni, Role of doping and CuO segregation in improving the giant permittivity of $CaCu_3Ti_4O_{12}$, Journal of Solid State Chemistry 177 (2004) 4494–4500.
[20] M.A. de la Rubia, P. Leret, J. de Frutos, J.F. Fernández, Effect of the synthesis route on the microstructure and the dielectirc behavior of $CaCu_3Ti_4O_{12}$ ceramics, Journal of the American Chemical Society 95 (2012) 1866–1870.
[21] X.L. Zhou, P.Y. Du, Effects of preparation on giant dielectric constant of $CaCu_3Ti_4O_{12}$ ceramics, Journal of Inorganic Materials 20 (2005) 484–488.
[22] J.Q. Huang, L.X. Hong, P.Y. Du, Dielectric properties of a three-phase Fe-Ni-$BaTiO_3$ composite, Acta Physica Sinica 55 (2006) 3664–3669.
[23] J.L. Zhang, P. Zheng, C.L. Wang, M.L. Zhao, J.C. Li, J.F. Wang, Dielectric dispersion of $CaCu_3Ti_4O_{12}$ ceramics at high temperatures, Applied Physics Letters 87 (2005) 142901-1–142901-3.
[24] Z.H. Chen, J.Q. Huang, Q. Chen, C.L. Song, G.R. Han, W.J. Weng, P. Y. Du, A percolative ferroelectric–metal composite with hybrid dielectric dependence, Scripta Materialia 57 (2007) 921–924.
[25] T.B. Adams, D.C. Sinclair, A.R. West, Influence of processing conditions on the electric properties of $CaCu_3Ti_4O_{12}$ ceramics, Journal of the American Ceramic Society 89 (2006) 3129–3135.
[26] T.B. Adams, D.C. Sinclair, A.R. West, Giant barrier layer capacitor effects in $CaCu_3Ti_4O_{12}$ ceramics, Advanced Materials 14 (2002) 1321–1323.
[27] S.F. Shao, J.L. Zhang, P Zheng, W.L. Zhong, C.L. Wang, Microstructure and electrical properties of $CaCu_3Ti_4O_{12}$ ceramics, Journal of Applied Physics 99 (2006) 084106-1–084106-11.
[28] S.R. Elliott, A.C. conduction in amorphous chalcogenide and pnictide semiconductors, Advances in Physics 36 (1987) 135–217.
[29] Z. Wang, X.M. Chen, L. Ni, Y.Y. Liu, X.Q. Liu, Dielectric relaxations and formation mechanism of giant dielectric constant step in $CaCu_3Ti_4O_{12}$ ceramics, Applied Physics Letters 90 (2007) 102905-1–102905-3.